

# Synthesis of tetracalcium phosphate from mechanochemically activated reactants and assessment as a component of bone cements

H. E. Romeo · M. A. Fanovich

Received: 20 April 2007 / Accepted: 5 February 2008 / Published online: 29 February 2008  
© Springer Science+Business Media, LLC 2008

**Abstract** The aim of this work was to gain a better understanding about the synthesis of tetracalcium phosphate (TTCP,  $\text{Ca}_4(\text{PO}_4)_2\text{O}$ ) through a solid-state reaction from mechanochemically activated  $\text{CaCO}_3\text{--}(\text{NH}_4)_2\text{HPO}_4$  mixtures. The evolution of the reaction was followed by DTA, XRD, FTIR and SEM techniques. An enhanced reactivity of the mixtures was detected as the mechanochemical treatment times increased. This effect was related to both the loss of crystallinity of the reactants and the production of defects on their surfaces. 6 h of mechanochemical processing at 1190 rpm, followed by 3 h of thermal treatment at 1500°C, were enough to obtain pure TTCP. The crystallinity and purity of the obtained TTCP were checked by XRD and FTIR. The morphologic characteristics were analyzed by SEM and BET analysis. The behavior of synthesized TTCP powder in combination with commercial dicalcium phosphate anhydrous (DCPA,  $\text{CaHPO}_4$ ), as the solid phase of bone cements, was tested. Both the combination of different particle sizes of TTCP and DCPA and the effect of different kinds of accelerator agents (disodium hydrogen phosphate, tartaric acid, citric acid and oxalic acid) on setting time and degree of conversion to hydroxyapatite (HA,  $\text{Ca}_{10}(\text{PO}_4)_6(\text{OH})_2$ ) were evaluated. The combination of TTCP (0.32 m<sup>2</sup>/g) with DCPA (1.52 m<sup>2</sup>/g), in a 1/1 molar ratio, showed the shortest setting times and high conversions to HA when an oxalic acid solution (5% volume fraction) was used as the liquid phase of the formulation. Results obtained from this work demonstrated that synthesized TTCP shows

promising behavior as a component of bone cements, exhibiting not only a smaller particle size than that usually reported but also a low degree of crystallinity, all of which increases the reactivity of the obtained TTCP. This study provided a very efficient method for synthesizing pure TTCP through a modified solid-state reaction from mechanochemically activated reactants, employing very short times of thermal treatment in comparison with the conventional processes.

## 1 Introduction

Brown and Chow [1] formulated a calcium phosphate cement (CPC) from tetracalcium phosphate (TTCP,  $\text{Ca}_4(\text{PO}_4)_2\text{O}$ ) and dicalcium phosphate anhydrous (DCPA,  $\text{CaHPO}_4$ ) or dicalcium phosphate dihydrate (DCPD,  $\text{CaHPO}_4 \cdot 2\text{H}_2\text{O}$ ). These components react in an aqueous environment to form, as the final product, hydroxyapatite (HA,  $\text{Ca}_{10}(\text{PO}_4)_6(\text{OH})_2$ ). The combination of setting and biocompatibility properties makes CPC a potentially useful material in a diversity of dental and medical applications. In the last two decades, numerous studies [2–7] were conducted to gain knowledge about the development of this CPC in the biomaterials area. However, very basic characteristics of the cements [8] are not well understood yet. The influence of many preparation variables on the final properties of the TTCP-DCPA based cements has been reported. The particle size of the calcium phosphate used and the phase composition of the cement paste are two of many key factors [9, 10] that have a great effect on the performance of CPC. It is known that mechanochemical treatment is one of the most versatile ways to modify the

H. E. Romeo (✉) · M. A. Fanovich  
Institute of Materials Science and Technology (INTEMA),  
University of Mar del Plata and National Research Council  
(CONICET), J. B. Justo 4302, 7600 Mar del Plata, Argentina  
e-mail: hromeo@fi.mdp.edu.ar

characteristics of the powders frequently employed in CPC systems [11, 12]. Camiré et al. have reported the influence of prolonged milling of  $\alpha$ -TCP on its crystallinity and reactivity [13] as well as other authors have investigated the possibility of controlling the final micro and nanostructural features of a  $\alpha$ -TCP-based cement by modifying the particle size of the starting powder by milling [14].

Different ways of synthesis of TTCP have been proposed, which invariably consist in solid-state reactions from mixtures of the reactants. This type of reaction requires long treatment times at high temperatures, and the obtained product is generally not pure. The product can be composed of mixtures of calcium phosphates; even calcium oxide can be present depending on the reactant nature and the synthesis conditions [15–19]. The reactivity of TTCP depends on both the manner in which it is produced and the subsequent treatments on it. Gbureck et al. [20, 21] have reported the effect of prolonged high-energy ball milling of TTCP on its crystallinity, reactivity and thermal behavior compared to unactivated and highly crystalline TTCP. Despite the numerous publications, only few works focus in detail on the synthesis of TTCP powder used in these CPC systems.

In this work, the synthesis of TTCP through a modified solid-state reaction between  $\text{CaCO}_3$  and  $(\text{NH}_4)_2\text{HPO}_4$  is described. The main modification introduced in the synthesis consisted in the mechanochemical activation of the reactants in alcoholic suspension. Analysis of the influence of mechanochemical treatment time on phase composition of the obtained products is reported. Furthermore, the characterization of the activated mixtures after different thermal treatments allowed the identification of intermediate phases formed during the reaction. The pure synthesized TTCP was used in the preparation and characterization of bone cements in combination with commercial DCPA. The influence of grinding time of TTCP and DCPA powders, Ca/P molar ratio and the hardening accelerator of the cement paste on setting time and conversion to HA was analyzed.

## 2 Materials and methods

### 2.1 Mechanochemical activation and reactivity of $\text{CaCO}_3$ – $(\text{NH}_4)_2\text{HPO}_4$ mixtures

Homogeneous mixtures of  $\text{CaCO}_3$  (Mallinckrodt) and  $(\text{NH}_4)_2\text{HPO}_4$  (Merck) with molar ratio Ca/P = 2 were prepared and mechanochemically activated in a planetary ball mill (Fritsch Pulverisette 7). Mechanochemical treatments were performed suspending the solid mixtures in two isopropyl alcohol solutions containing 0.05% (series A)

and 0.2% (series B) of distilled water respectively, during measured times between 1 and 10 h at 1190 rpm. The samples were named A-treatment time (in hours) (A1, A6, ..., A10) and B-treatment time (in hours) (B1, B6, ..., B10) respectively. Zirconia vials were used for the mechanochemical treatment, keeping constant the angular velocity of the mill, the milling media mass/solid mass (6.4) and the solid mass/alcohol volume (0.35 g/ml) ratios. After each mechanochemical treatment, the samples were dried at 80°C and analyzed by X-ray diffraction (XRD) and differential thermal analysis (DTA). The thermally treated samples were also characterized by Fourier transformed infrared (FTIR) spectroscopy.

The mixture activated during 6 h (A6) was thermally treated up to 80°, 850°, 1320°, 1400° and 1500°C and cooled at room temperature in order to identify, by XRD and FTIR analysis, the intermediate phases produced during the formation of TTCP. The optimal activation time and temperature for the synthesis of pure TTCP from  $\text{CaCO}_3$ – $(\text{NH}_4)_2\text{HPO}_4$  mixtures were established.

In order to evaluate the effect of the mechanochemical treatment on the obtained product, two comparative syntheses were accomplished from samples A6 and A0, employing the same experimental conditions. For this purpose, the mixtures were heated at 1500°C for 3 h in an electric high-temperature furnace (Carbolite RHF 17/6S) and then cooled at room temperature. The obtained powders were characterized by XRD and scanning electron microscopy (SEM).

### 2.2 Milling processes of TTCP and DCPA powders

TTCP powder was prepared from sample A6 after 3 h of thermal treatment at 1500°C, as described above. The DCPA powder was a commercial reagent-grade chemical (Aldrich). The TTCP and DCPA powders were separately milled in a planetary ball mill (Fritsch Pulverisette 7) to reduce the mean particle size, for 30 min and 5 h, at 890 rpm, using free-water isopropyl alcohol as a suspending solvent, milling media mass/solid mass (6.4) and solid mass/alcohol volume (0.35 g/ml) ratios. The TTCP and DCPA powders, with different particle sizes, were characterized by XRD, SEM and then employed to analyze the influence of particle size on the setting process. The BET method was used to determine the specific surface area (SSA) of the calcium phosphates.

### 2.3 Preparation of calcium phosphate cements

The CPCs consisted of a solid phase containing a mixture of TTCP and DCPA and a liquid phase formed by an

aqueous solution of a hardening accelerator (disodium hydrogen phosphate, tartaric acid, citric acid or oxalic acid). Two TTCP/DCPA molar ratios prepared by hand mixing in an agate mortar were used. Some formulations were made from milled TTCP and DCPA powders. Cement pastes were prepared by mixing 1.3 g of solid phase and the required amount of liquid phase to obtain a workable paste in a PTFE vessel. Then, the pastes were poured into a polystyrene mould, 11.4 mm diameter and 5 mm height. The filled moulds were stored at 37°C and 100% relative humidity (RH). In each case the initial and final setting times (I and F) were determined with Gillmore needles. The setting times, obtained from a set of three samples of each cement, are expressed as mean  $\pm$  standard error of the mean. Statistical analysis was performed on the experimental values by means of a Student-*t*-test. After 24 h of incubation time at 37°C and 100% RH, the hardened specimens were removed from the moulds for characterization by XRD and FTIR. Fracture surfaces of the developed CPCs were observed by SEM.

#### 2.4 Characterization techniques

XRD patterns were recorded on a Philips PW 1830/00 diffractometer, using Ni-filtered Cu K $\alpha$  radiation at 40 kV and 30 mA. The  $2\theta$  range from 10° to 60° was covered at scan speed of 1°min<sup>-1</sup> on powdered samples.

The thermal behavior of the mechanochemically activated mixtures was studied by differential thermal analysis (DTA, Shimadzu DTA-50H analyzer) up to 1500°C, using a heating rate of 10°C min<sup>-1</sup>.

Fourier transformed infrared (FTIR) spectra were recorded with a Bruker IFS 25 spectrometer in the transmission mode, in the range of 400–4000 cm<sup>-1</sup> with a resolution of 2 cm<sup>-1</sup>. Spectra were obtained using pellets of the samples with spectroscopic-grade KBr.

The calcium phosphate powders as well as the fracture surfaces of the CPCs were observed by scanning electron microscopy (SEM, Jeol JXA-8600) after coating the samples with a thin gold layer.

The specific surface areas (SSA) were measured by nitrogen adsorption and desorption on the particle surface with a Micromeritics Flowsorb II 2300 device.

The initial (I) and final (F) setting times of the developed cements were determined with Gillmore needles according ASTM standard C266-99. “Standard test method for time of setting of hydraulic cement paste by Gillmore needles, ASTM International 2002”.

### 3 Results and discussion

#### 3.1 Effect of mechanochemical treatment on mixtures of CaCO<sub>3</sub> and (NH<sub>4</sub>)<sub>2</sub>HPO<sub>4</sub>

It is known that the use of high-energy milling produces the reduction in the particle size, but in addition the impact and friction effects lead to structural changes associated with the amorphization of the crystal lattice [22]. These observations agree with the interpretation of the mechanochemical treatment as a progressive deterioration of the original crystalline structure, with production of extended defects and, in some cases, partial decomposition of the solid. The mechanochemical process can be interpreted as proceeding through two processes that cannot be separated: The production of textural changes which can be detected by microscopy examination, and the alteration in the chemical-structural properties of the material. Although both processes occur simultaneously, the latter arises from the formation of particles containing high superficial energy. This process is distinguished from a thermal process, since the influence of temperature variations occurs in the totality of the solid mass, whereas a mechanochemical process produces energetic alterations in restricted surface regions of the solid. The materials obtained by this process do not have similar properties as those produced by thermal methods [22]. On the contrary, the stresses created in the solid are enough to modify its structure and to lower the internal order. As a result of this process, the production of defects and the loss of crystallinity bring along an increase in the reactivity of the solids.

Results from the present study show that the mechanochemical treatment produces significant effects on reactivity of CaCO<sub>3</sub>–(NH<sub>4</sub>)<sub>2</sub>HPO<sub>4</sub> mixtures. Table 1 lists the crystalline phases present in activated mixtures as determined by XRD for series A.

The main phases detected in the mechanochemically treated mixtures were CaCO<sub>3</sub> and NH<sub>4</sub>H<sub>2</sub>PO<sub>4</sub>. After 1 h of treatment, only a small quantity of crystalline (NH<sub>4</sub>)<sub>2</sub>HPO<sub>4</sub> was detected. The same behavior was observed for series B (0.2% water). This observation indicates that most of the initial (NH<sub>4</sub>)<sub>2</sub>HPO<sub>4</sub> was decomposed during the first hour of treatment, losing about 50% of its ammonium ion content, and transforming into NH<sub>4</sub>H<sub>2</sub>PO<sub>4</sub>. Furthermore, this decomposition was evidenced by the NH<sub>3</sub> liberated when the vials were opened. On the other hand, as the time of treatment increased, the crystallinity of CaCO<sub>3</sub> and NH<sub>4</sub>H<sub>2</sub>PO<sub>4</sub> decreased. The measurement of X-ray diffracted intensities showed this effect in both series of samples. The crystallinity of both calcium carbonate and

**Table 1** Crystalline phases determined on activated mixtures

Sample	Time of mechanochemical treatment (h)	Identified phases
A0	–	CaCO <sub>3</sub> , (NH <sub>4</sub> ) <sub>2</sub> HPO <sub>4</sub>
A1	1	CaCO <sub>3</sub> , NH <sub>4</sub> H <sub>2</sub> PO <sub>4</sub> , (NH <sub>4</sub> ) <sub>2</sub> HPO <sub>4</sub> trace
A6	6	CaCO <sub>3</sub> , NH <sub>4</sub> H <sub>2</sub> PO <sub>4</sub>
A10	10	CaCO <sub>3</sub> , NH <sub>4</sub> H <sub>2</sub> PO <sub>4</sub>

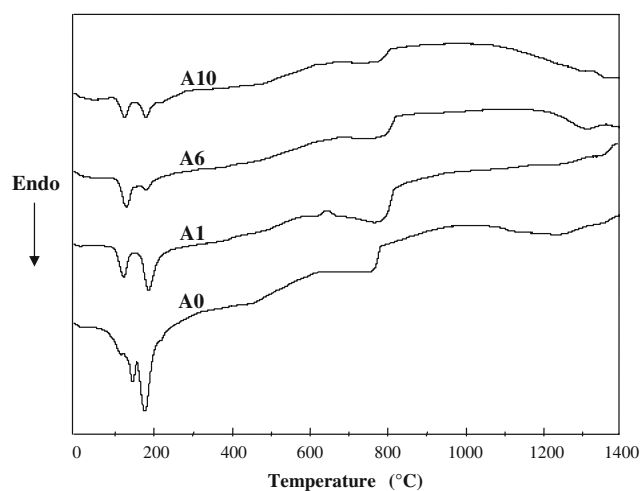
ammonium dihydrogen phosphate decreased about 50% from their initial values in mixtures milled for 10 h.

Moreover, the formation of a crystalline (NH<sub>4</sub>)<sub>2</sub>Ca(HPO<sub>4</sub>)<sub>2</sub>·H<sub>2</sub>O phase was detected by XRD in samples of series A treated for 4 and 5 h but not in series B. However, the presence of this crystalline phase did not produce any differences in the formation of TTCP. The development of this phase was probably favoured by both the low water content and the increased homogeneity of the reactants, however, as the treatment time increased, this phase disappeared from the samples.

### 3.1.1 Thermal analysis of the activated mixtures

Figure 1 shows the DTA diagrams of series A. The endothermic bands observed in the range of 100–300°C and 700–850°C were attributed to the decomposition reactions of the reactants whereas the endothermic band at about 1300–1400°C was attributed to the formation of TTCP.

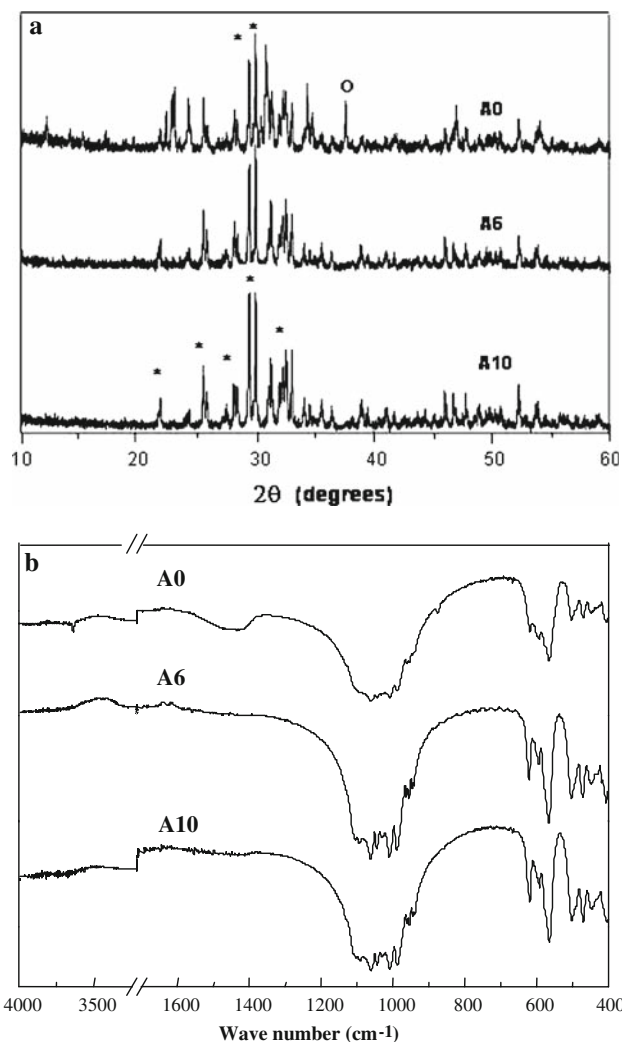
The bands observed at temperatures below 600°C are due to the decomposition of the ammonium phosphates. The bands corresponding to the decomposition of (NH<sub>4</sub>)<sub>2</sub>HPO<sub>4</sub> are observed at the lowest temperature and those bands due to fusion of NH<sub>4</sub>H<sub>2</sub>PO<sub>4</sub> appeared between

**Fig. 1** Differential thermal analysis of series A (0.05% water)

206 and 190°C [23]. Moreover, an endothermic band was observed between 700 and 850°C, which corresponds to the decomposition of CaCO<sub>3</sub>. By increasing the mechanochemical treatment time, the area of the band is reduced, in agreement with the lower intensities detected by XRD for CaCO<sub>3</sub> peaks. In the high temperature range, endothermic bands at about 1300 and 1400°C were detected, which could be attributed to the first formation of TTCP in samples A6 and A10.

Figure 2a and b show the XRD and FTIR spectra of series A after dynamic thermal treatment (10°C min<sup>-1</sup>) up to 1500°C.

The analysis of the diffraction peaks revealed that the intensity corresponding to the TTCP phase was the highest in sample A10 and followed the sequence A10 > A6 ≫ A0. The free CaO content decreased with the milling time. From these results, it can be seen that the formation of

**Fig. 2** Characterization of samples A0, A6 and A10 after dynamic thermal treatment up to 1500°C: (a) XRD diagrams (\*TTCP, °CaO) and (b) FTIR spectra

TTCP was completed for A6 and A10 samples. The proposed TTCP synthesis was significantly easier than others due to the mechanochemical activation of the reactants.

Figure 2b shows the FTIR spectra of samples A0, A6 and A10. The thermal treatment up to 1500°C produced a slight formation of TTCP in sample A0 (without mechanochemical treatment). The FTIR spectrum of this sample shows that it still contains CaO. This fact is indicated by the OH band at 3648 cm<sup>-1</sup>, due to superficial Ca(OH)<sub>2</sub> formed through absorption of water by CaO [24]. Furthermore, the bands observed at 1400–1500 and 868 cm<sup>-1</sup> evidence the presence of CO<sub>3</sub><sup>2-</sup> in the sample. The FTIR peak assignment corresponding to the TTCP phase is based on previous publications [15, 25]. FTIR spectra of samples activated for long periods of time (A6 and A10) showed only the absorption bands expected for pure TTCP in the 4000–400 cm<sup>-1</sup> range. These results demonstrate that 6 h of mechanochemical treatment of the starting mixture are enough to obtain pure TTCP by dynamic thermal treatment (10°C min<sup>-1</sup>) up to 1500°C.

### 3.1.2 Evolution of the reaction in sample A6 and characterization of synthesized TTCP

In order to study the thermal evolution of the reaction from mixtures activated for 6 h, XRD and FTIR analysis were performed.

Figure 3 shows the FTIR spectra of sample A6 treated at different temperatures. As stated above, only CaCO<sub>3</sub> and NH<sub>4</sub>H<sub>2</sub>PO<sub>4</sub> are present in sample A6 dried at 80°C. The XRD analysis (Table 2) of sample A6–850 shows the presence of β-TCP, CaCO<sub>3</sub> and carbonate apatite. The FTIR spectrum of this sample confirms that CO<sub>3</sub><sup>2-</sup> occupy the OH<sup>-</sup> positions in the apatite structure, due to the absence of the band at 3575 cm<sup>-1</sup>, assigned to OH<sup>-</sup> in the apatite structure. This analysis suggests that already at 850°C the mixture of reactants begins to react. However, it must be taken into account that this temperature could be different for samples activated during diverse times as well as at different angular velocities during milling. The first formation of TTCP was detected on sample A6 treated at 1320°C. Moreover, this sample still contained HA and CaO, while β-TCP was not detected. The FTIR spectrum corresponding to sample A6-1320 shows the characteristic bands of TTCP together with those of Ca(OH)<sub>2</sub> from hydrated CaO (3648, 1400–1550, and 868 cm<sup>-1</sup>) and the OH<sup>-</sup> stretching band at 3570 cm<sup>-1</sup>. On the other hand, sample A6-1400 is composed of CaO, HA and TTCP (Table 2 and Fig. 3). It was observed that the FTIR band at 3570 cm<sup>-1</sup> increased due to OH<sup>-</sup> stretching in HA structure, and the band at 3648 cm<sup>-1</sup> due to Ca(OH)<sub>2</sub> decreased with respect to sample A6-1320. This fact might be

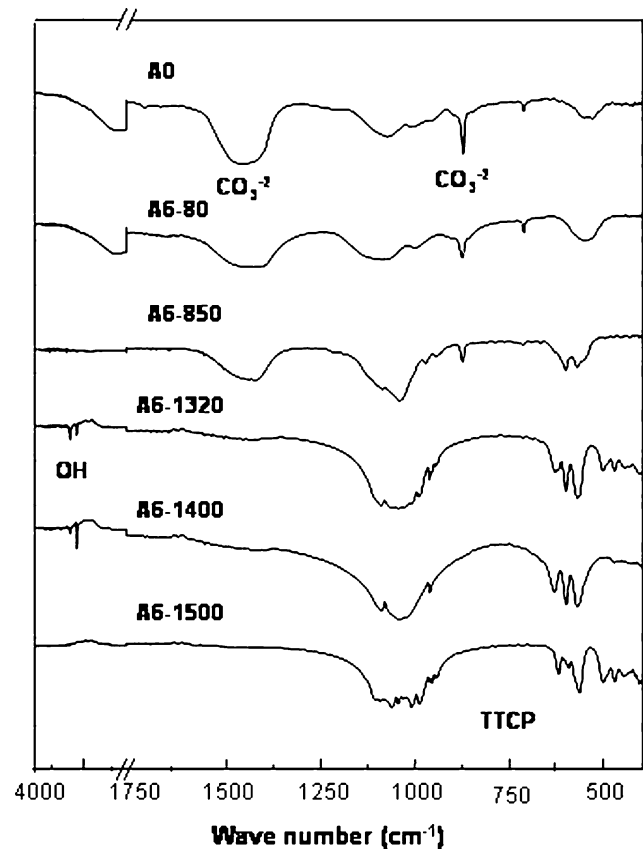


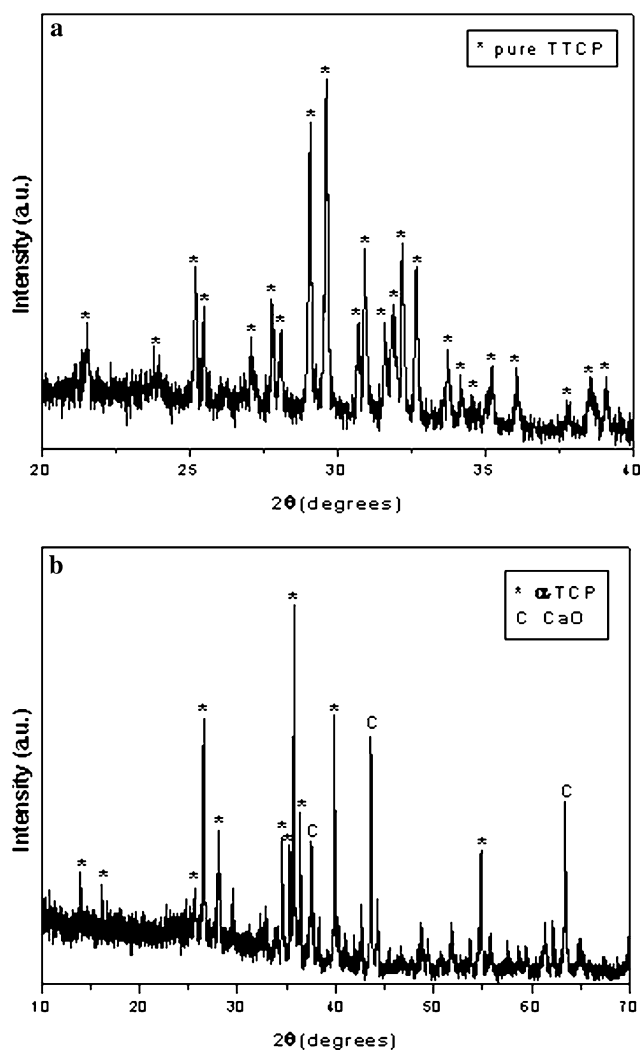
Fig. 3 FTIR spectra of sample A6 after different thermal treatments

Table 2 Products detected by XRD on sample A6 after different thermal treatments

Sample	T (°C)	Phase composition
A6-80	80	CaCO <sub>3</sub> > NH <sub>4</sub> H <sub>2</sub> PO <sub>4</sub>
A6-850	850	β-Ca <sub>3</sub> (PO <sub>4</sub> ) <sub>2</sub> , CaCO <sub>3</sub> > CO <sub>3</sub> -HA
A6-1320	1320	HA > TTCP > CaO
A6-1400	1400	HA > CaO ≫ TTCP
A6-1500	1500	TTCP

attributed to a partial hydrolysis of TTCP with production of HA. The A6-1500 sample consisted of pure TTCP, as identified by XRD and FTIR. Neither OH<sup>-</sup> nor CO<sub>3</sub><sup>2-</sup> ions were detected in this sample. It must be kept in mind that these results were obtained without keeping the reaction mixture for long times at the maximum temperature. For this reason, it should be possible to synthesize pure TTCP by using isothermal treatments at temperatures lower than 1500°C.

In order to evaluate the effect of the mechanochemical treatment on the product obtained from samples A6 and A0, after 3 h of thermal treatment at 1500°C, XRD analysis were accomplished.



**Fig. 4** XRD diffractograms corresponding to (a) pure TTCP and (b) product obtained from sample A0 after 3 h of thermal treatment at 1500°C

The product obtained from the mechanochemically activated sample (A6) consisted of high-purity TTCP (Fig. 4a) and showed a mean particle size (about 5  $\mu\text{m}$ ) smaller than that obtained, after milling, by other methods [6, 17]. On the other hand, a biphasic product consisting on CaO and  $\alpha$ -TCP was obtained from the A0 sample (Fig. 4b). In this way, the studied synthesis provides a new route of preparation of pure TTCP by using mechanochemical activation of the reactants, employing less time of thermal treatment in comparison to currently known methods.

### 3.2 Characterization of milled TTCP and DCPA powders

Figure 5 shows the effect of milling processes on TTCP and DCPA powders by XRD analysis and SEM

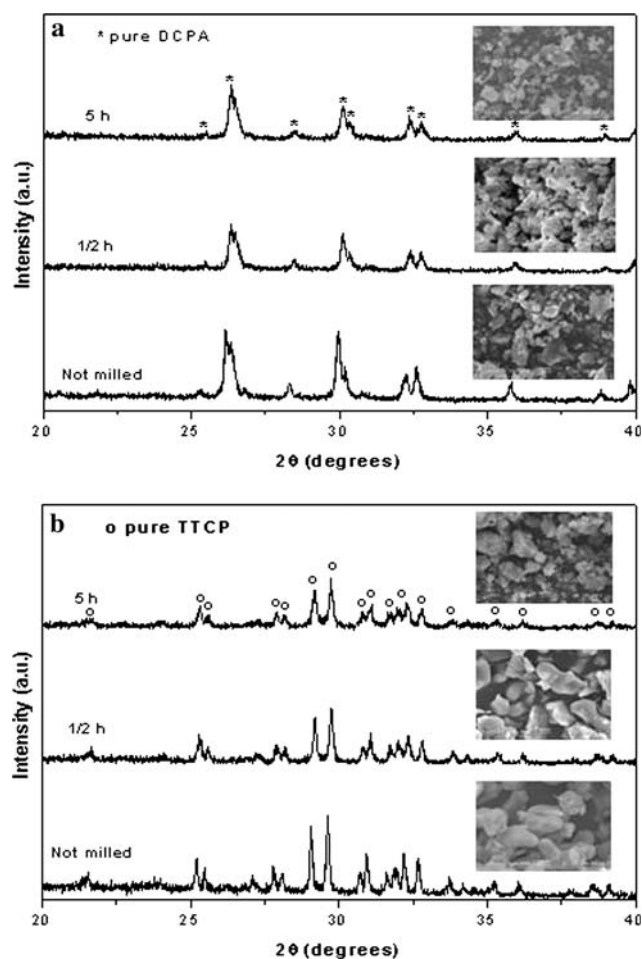


**Fig. 5** XRD analysis and SEM observations on milled: (a) DCPA, (b) TTCP powders

observations. Unmilled DCPA powder presents irregular crystals with a mean particle size of about 2  $\mu\text{m}$ . Synthesized TTCP powder exhibits more spherical particles than DCPA, with a mean particle size of about 5  $\mu\text{m}$  as determined by image analysis. A progressive reduction in particle size was observed for TTCP and DCPA samples, as the milling time increased. The DCPA and TTCP mean particle sizes showed a reduction in their initial values of 55% and 46% respectively, after 5 h milling. Reduction in the degree of crystallinity of TTCP and DCPA phases was detected by XRD. Table 3 shows the specific surface areas measured by the BET method as well as the different formulations of the prepared cements.

### 3.3 Evaluation of synthesized TTCP in CPC formulations

The structural relationship between monoclinic TTCP and hexagonal HA allows the formation of a thin HA layer on the surface of TTCP when water is present in the

**Table 3** Characteristics of the prepared cements

Sample	TTCP/DCPA molar ratio	SSA (m <sup>2</sup> /g)		Powder/liquid ratio (g/ml)	Liquid phase composition	Setting time (min) (S.T.)	
		TTCP	DCPA			I	F
CPC-A	1/1	0.32	1.52	3	Na <sub>2</sub> HPO <sub>4</sub> (2% volume fraction)	44 ± 2	180 ± 2
CPC-B	1/2	0.32	1.52	3	Na <sub>2</sub> HPO <sub>4</sub> (2% volume fraction)	30 ± 1	57 ± 1
CPC-C	1/1	0.32	6.66	2.6	Na <sub>2</sub> HPO <sub>4</sub> (2% volume fraction)	>300	–
CPC-D	1/1	1.88	1.52	2.6	Na <sub>2</sub> HPO <sub>4</sub> (2% volume fraction)	40 ± 1	98 ± 2
CPC-E	1/1	0.32	1.52	3	Na <sub>2</sub> HPO <sub>4</sub> (5% volume fraction)	11 ± 1	39 ± 4
CPC-F	1/2	0.32	1.52	3	Na <sub>2</sub> HPO <sub>4</sub> (5% volume fraction)	12 ± 3	31 ± 3
CPC-G	1/1	0.32	1.52	2.6	Tartaric acid (5% volume fraction)	48 ± 2	90 ± 3
CPC-H	1/2	0.32	1.52	2.6	Tartaric acid (5% volume fraction)	38 ± 2	65 ± 3
CPC-I	1/1	0.32	1.52	3	Citric acid (5% volume fraction)	19 ± 2	127 ± 5
CPC-J	1/2	0.32	1.52	3.25	Citric acid (5% volume fraction)	15 ± 1	62 ± 4
CPC-K	1/1	0.32	1.52	2.24	Oxalic acid (5% volume fraction)	12 ± 1	20 ± 1
CPC-L	1/2	0.32	1.52	2.45	Oxalic acid (5% volume fraction)	12 ± 1	23 ± 2

environment. This event may produce a passive TTCP surface that shows low reactivity when used in hydraulic pastes [9, 20, 26]. The low reaction rate would be related to diffusive processes through the HA layer. The hydration reaction assumed for TTCP takes place according to Eq. 1 [27]:

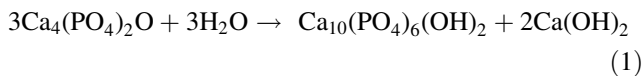


Figure 4a shows the XRD patterns corresponding to a pure TTCP phase, in agreement with the Standard Data N° 70-1379. The synthesized TTCP did not evidence any detectable hydrolysis processes before using it in CPCs formulations. The characteristic signals of Ca(OH)<sub>2</sub> were not detected. However, we believe that the formation of an undetectable thin low-crystallinity HA layer onto TTCP particles cannot be rejected. This conjecture is based on the results of the initial and final setting times measured for the developed CPCs (Table 3). Comparing the setting times of samples CPC-A and CPC-D, we observed that when the SSA of TTCP powder increases from 0.32 to 1.88 m<sup>2</sup>/g (keeping constant the SSA of DCPA), the I decreases slightly whereas the F of the CPC decreases about 45%. Gbureck et al. [20] reported setting experiments on mechanochemically activated TTCP-water cements. They observed that the hardening time decreased with milling time from ~5–6 h (1 h milling) to ~2 h (24 h milling). This effect was assigned to crystal size reduction and the formation of an amorphous phase. We consider that in TTCP–DCPA systems the reduction in TTCP crystal size is not effective in reducing considerably the cement setting time unless the reduction is accompanied by loss of crystallinity. On the other hand, the reduction in DCPA particle size (keeping constant the SSA of TTCP) was not successful to lower

the initial and final setting times (see samples CPC-A and CPC-C), due possibly to the large fraction of the required liquid phase to form the paste.

A strong reduction in both I and F, when a TTCP/DCPA = 1/2 molar ratio was employed in the solid phase, was observed comparing samples CPC-A and CPC-B. This effect would be associated to the preferential dissolution of the acidic component (DCPA) of the solid phase when an alkaline solution is used as the liquid phase of the formulation.

As can also be seen from Table 3, a change from 2% to 5% volume fraction in the concentration of the Na<sub>2</sub>HPO<sub>4</sub> solution led to a significant reduction in both setting times (see CPC-A and CPC-E cements). For this reason, in order to study the effect of different accelerators on setting time, a liquid phase concentration of 5% volume fraction was fixed.

Figure 6 shows the XRD patterns of the CPCs after 24 h of incubation time at 37°C and 100% RH. Conversion to low-crystallinity HA was clearly observed in CPC-E, CPC-K and CPC-L samples. A significant decrease in the intensities of TTCP peaks when oxalic acid solution was used as the liquid phase (CPC-K and CPC-L) was observed.

Chow et al. [9] studied the hydrolysis of TTCP under different conditions. They showed that TTCP hydrolysis is affected by the solution pH and the particle size of the powder. In this work we proposed different accelerator agents with the objective to change the pH of the liquid phase used in the CPCs (Table 3). The influence of disodium hydrogen phosphate, tartaric acid, citric acid and oxalic acid solutions (5% volume fraction) on setting time (Table 3) and degree of conversion to HA (Fig. 6) from TTCP (0.32 m<sup>2</sup>/g) and DCPA (1.52 m<sup>2</sup>/g) mixtures as solid phases of the cements, was evaluated.

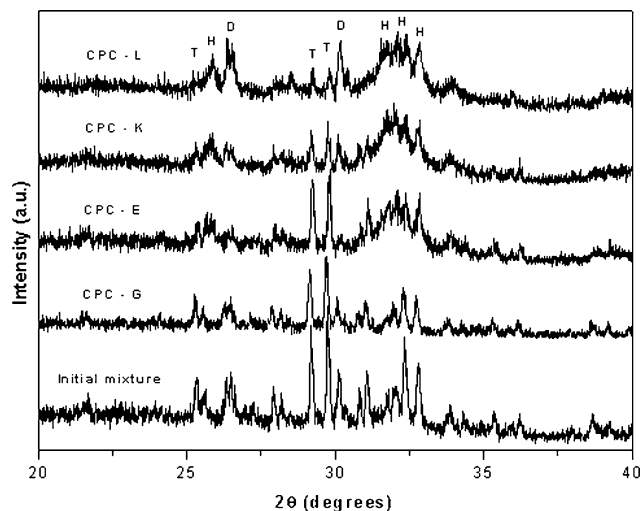


**Fig. 6** XRD analysis of different cements after setting at 37°C and 100% RH for 24 h. References: D (DCPA), T (TTCP) and H (HA)

The CPC-I and CPC-J formulations, containing a citric acid solution as the liquid phase, showed acceptable initial setting times; however, they led to the formation of low-consistence solids after setting.

We observed that by using liquid phases with different pH, we may facilitate the specific dissolution of some of the two calcium phosphates of the solid mixture. In this way, the use of a  $\text{Na}_2\text{HPO}_4$  solution (pH = 9.2) helped the specific dissolution of DCPA, the acidic component of the

cement. The XRD spectrum corresponding to the set CPC-E sample (Fig. 6) shows this effect as well as the formation of low-crystallinity HA. As can be seen from the diffraction patterns corresponding to the TTCP phase, this calcium phosphate remains practically unreacted in this cement.

On the other hand, when an oxalic acid solution is used as a liquid phase (pH = 0.6), the dissolution of TTCP, the basic component of the cement, is favored. Figure 6 shows the decrease of the intensities of TTCP peaks in XRD spectra corresponding to the CPC-K and CPC-L cements. Setting times (I and F) were not substantially modified when TTCP/DCPA = 1/2 molar ratio was used in the solid phase. This fact agrees with the specific dissolution of TTCP when an acid solution is used in the formulation. The use of oxalic acid as a setting accelerator led to the shortest setting times and high conversions to low-crystallinity HA.

No detectable conversion to HA was observed when tartaric acid was employed as an accelerator (Fig. 6, sample CPC-G). We associate this to the formation of amorphous calcium tartrates which were detected by FTIR analysis (not shown). These precipitates could be deposited on reactant surfaces hindering the conversion to HA.

Figure 7 shows the fracture surfaces of cements set using different accelerators. When tartaric acid was used (Fig. 7a), a non-homogeneous structure was developed showing different phases with a low degree of

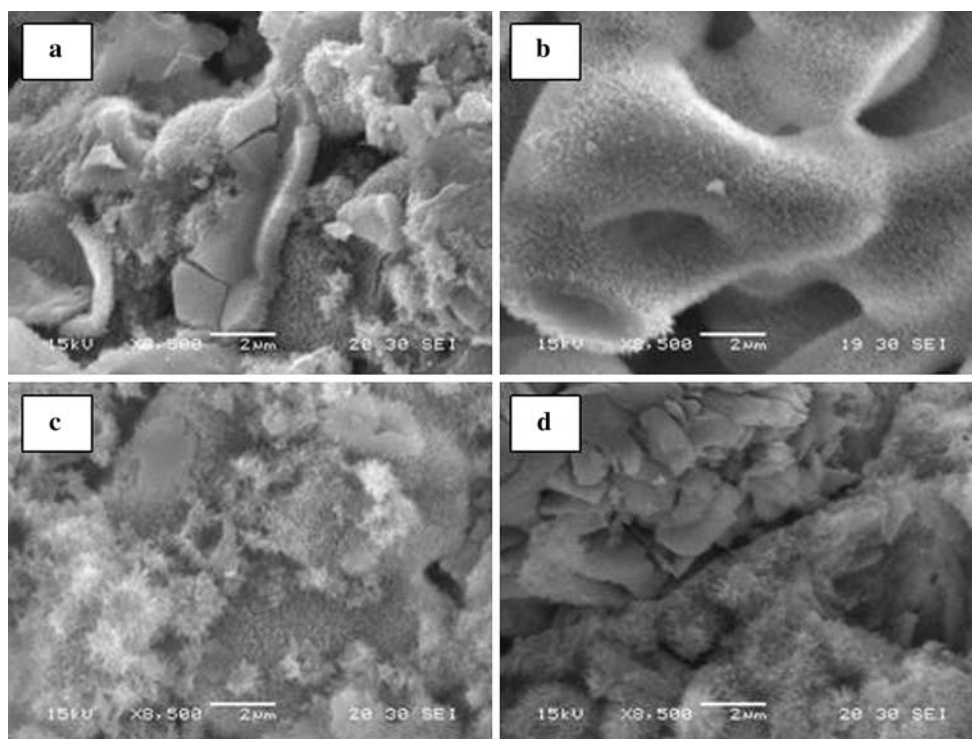


**Fig. 7** SEM photographs of cement fracture surfaces, (a) CPC-G, (b) CPC-E, (c) CPC-K and (d) CPC-L



entanglement. This is in agreement with the low mechanical resistance detected when samples were removed from the moulds. On the other hand, very small HA crystals were observed on the fracture surface of the cement prepared from  $\text{Na}_2\text{HPO}_4$  solution as the liquid phase (Fig. 7b, sample CPC-E). These microcrystals would probably precipitate on the surface of TTCP particles, taking into account that in this system the DCPA particles are initially dissolved and the TTCP remains practically unreacted, which is in agreement with XRD analysis. As the micrograph shows, this cement evidenced the largest mean pore size in comparison with the other samples.

The best microstructure was observed when an oxalic acid solution and a TTCP/DCPA = 1/1 molar ratio were used (Fig. 7c). A homogeneous microstructure, with both a larger HA crystal size and a higher degree of entanglement than those corresponding to the other samples, was observed. However, in this case a smaller mean pore size is clearly noticed with respect to CPC-E cement. On the other hand, microstructural inhomogeneities were observed in sample CPC-L (Fig. 7d) which were attributed to the presence of unreacted DCPA particles, in agreement with the corresponding XRD spectrum.

It is very important to note that the systems developed in this work are simpler than those frequently reported in the literature. The proposed formulations contain neither HA crystal seeds [28], nor fibers [7], nor gelling agents [3] as components. Despite this, short setting times and high conversions to HA were obtained for the bone CPCs developed in this study from  $\text{Na}_2\text{HPO}_4$  and oxalic acid solutions.

A more detailed microstructural analysis, employing characterization techniques based on electrical measurements, is in progress.

#### 4 Conclusions

A very efficient method for the synthesis of pure TTCP ( $\text{Ca}_4(\text{PO}_4)_2\text{O}$ ) through a modified solid-state reaction from mechanochemically activated  $\text{CaCO}_3$ – $(\text{NH}_4)_2\text{HPO}_4$  mixtures was developed. Mixtures with good homogenization and reduced crystallinity were obtained by mechanochemical treatment. In this way, very reactive blends of  $\text{CaCO}_3$  and  $\text{NH}_4\text{H}_2\text{PO}_4$  can be prepared with 6 h of processing at 1190 rpm. The enhanced reactivity of the mixtures was related to both the loss of crystallinity of the reactants and the production of defects on their surfaces. It was established that 3 h of thermal treatment at  $1500^\circ\text{C}$  were enough to obtain pure TTCP with small particle size from the mixture mechanochemically activated for 6 h.

The behavior of synthesized TTCP in combination with commercial DCPA, as the solid phase of bone cements,

was evaluated. Twelve formulations prepared using different accelerator agents, TTCP/DCPA molar ratios, specific surface areas of powders and powder/liquid ratios, were analyzed. The setting times were greatly reduced and a high conversion to low-crystallinity HA was attained when an oxalic acid solution (5% volume fraction) was employed as the liquid phase of the cements. This study provided a new route of preparation of TTCP through a solid-state reaction by using mechanochemical activation of the reactants. Results obtained from this work demonstrated that synthesized TTCP exhibits not only a smaller particle size than that usually reported but also a low degree of crystallinity. All of this leads to an increase of the reactivity of the obtained TTCP. As a result, synthesized TTCP can be used as a component of bone cements with promising behavior for bone repair in dental and medical applications.

**Acknowledgements** The financial support of the following institutions is gratefully acknowledged: National Research Council (CONICET, Argentina), National Agency for the Promotion of Science and Technology (ANPCyT, Argentina, PICT 12-14593), University of Mar del Plata and Fundación Antorchas (Argentina).

#### References

1. B.W. Brown, L.C. Chow, *Dental Restorative Cement Paste*. US Patent No. 4.518.430, 1985
2. S. Matsuya, S. Takagi, L.C. Chow, *J. Mater. Sci: Mater. Med.* **11**, 305 (2000)
3. L.E. Carey, H.H.K. Xu, C.G. Simon, S. Takagi, L.C. Chow, *Biomaterials* **26**, 5002 (2005)
4. H.H.K. Xu, L.E. Carey, C.G. Simon Jr., S. Takagi, L.C. Chow, *Dent. Mat.* **23**, 433 (2007)
5. Y. Fukase, E.D. Eanes, S. Takagi, L.C. Chow, W.E. Brown, *J. Dent. Res.* **69**, 1852 (1990)
6. H.H.K. Xu, C.G. Simon Jr, *Biomaterials* **26**, 1337 (2005)
7. H.H.K. Xu, J.B. Quinn, *Biomaterials* **23**, 193 (2002)
8. M. Bohner, U. Gbureck, J.E. Barralet, *Biomaterials* **26**, 6423 (2005)
9. L.C. Chow, M. Marcovic, S.A. Frukhtbeyn, S. Takagi, *Biomaterials* **26**, 393 (2005)
10. C. Liu, H. Shao, F. Chen, H. Zheng, *Biomaterials* **24**, 4103 (2003)
11. S. Serraj, P. Boudeville, B. Pauvert, A. Terol, *J. Biomed. Mat. Res.* **55**, 566 (2001)
12. S. Serraj, P. Boudeville, A. Terol, *J. Mater. Sci: Mater. Med.* **12**, 45 (2001)
13. C.L. Camiré, U. Gbureck, W. Hirsiger, M. Bohner, *Biomaterials* **26**, 2787 (2005)
14. M.P. Ginebra, F.C.M. Driessens, J.A. Planell, *Biomaterials* **25**, 3453 (2004)
15. Y. Sargin, M. Kizilyalli, C. Telli, H. Güler, *J. Eur. Ceram. Soc.* **17**, 963 (1997)
16. V.V. Samuskevich, N.K. Belous, L.N. Samuskevich, *J. Inorg. Mat.* **39**, 520 (2003)
17. J.E. Barralet, L. Grover, T. Gaunt, A.J. Wright, I.R. Gibson, *Biomaterials* **23**, 3063 (2002)
18. A. Hoshikawa, N. Fukui, A. Fukuda, T. Sawamura, M. Hattori, K. Nakamura, H. Oda, *Biomaterials* **24**, 4967 (2003)
19. D. Guo, K. Xu, X. Zhao, Y. Han, *Biomaterials* **26**, 4073 (2005)

20. U. Gbureck, J.E. Barralet, M. Hofmann, R. Thull, J. Am. Ceram. Soc. **87**, 311 (2004)
21. U. Gbureck, M.P. Hofmann, J.E. Barralet, J. Am. Ceram. Soc. **88**, 1327 (2005)
22. A.W. Weeber, H. Bakker, Condens Matter **153**, 93 (1988)
23. R.C. Weast (ed.), *Handbook of Chemistry and Physics* (CRC Press, Boca Raton, FL, USA, 1976)
24. A. Slosarczyk, C. Paluszkiewicz, M. Gawlicki, Z. Paszkiewicz, Ceram. Int. **23**, 297 (1997)
25. U. Posset, E. Locklin, R. Thull, W. Kiefer, J. Biomed. Mater. Res. **40**, 640 (1998)
26. I. Martin, P.W. Brown, Adv. Cem. Res. **5**, 115 (1993)
27. L.L. Hench, *Handbook of Bioactive Ceramics*, vol. II (CRC Press, Boca Raton, USA, 1990)
28. C.S. Liu, W. Shen, J. Mater. Sci.: Mater. Med. **8**, 803 (1997)